

DYNAMICS OF ADJACENT STRUCTURES DURING HORIZONTAL GROUND MOTION

Miodrag Žigić¹
Nenad Grahovac²
Boris Brkić³

UDK: 624.042.7

DOI: 10.14415/konferencijaGFS2018.014

Summary: *We analyzed two adjacent structures connected by a friction element to each other. Both structures consist of two blocks and a viscoelastic damper, which is modeled by the fractional Zener model. The friction force within the friction element is described by the Coulomb friction law in a set-valued form. Horizontal ground motion induces movement of both structures which can cause a destroying pounding effect. Energy brought to the system consisting of two structures connected by a friction damper dissipates by work done by viscoelastic and friction forces. Ground excitation is modeled by a simplified earthquake model by means of Ricker's waves.*

Keywords: *adjacent structures, earthquake, dry friction, viscoelasticity*

1. INTRODUCTION

Lateral collisions of adjacent structures caused by earthquake excitation are known as structural pounding. Due to increased urbanization, buildings are often built very close to each other, which can result in their interaction during ground motion.

The survey on building pounding caused by 1989 Loma Prieta earthquake and distribution of pounding damage is presented in [1]. Analytical and numerical modeling studies on pounding effects during earthquakes can be found in [2]-[5].

Prevention of earthquake induced pounding between adjacent structures by using polymer elements is analyzed in [6]. Treatment of pounding between neighboring structures using Buckingham's Π theorem is presented in [7].

Mate et al. performed comparative study of various existing linear and non-linear simulation models for pounding on three adjacent single-degree-freedom and multi-degree-freedom linear elastic structures, see [8].

Seismic control performance for pounding tuned mass damper based on viscoelastic pounding force is presented in [9].

¹ Miodrag Žigić, University of Novi Sad, Faculty of Technical Sciences, Novi Sad, Trg Dositeja Obradovića 6, Novi Sad, Serbia, tel: ++381 21 485 2240, e – mail: mzigic@uns.ac.rs

² Nenad Grahovac, University of Novi Sad, Faculty of Technical Sciences, Novi Sad, Trg Dositeja Obradovića 6, Novi Sad, Serbia, tel: ++381 21 485 2240, e – mail: ngraho@uns.ac.rs

³ Boris Brkić, University of Novi Sad, Faculty of Technical Sciences, Novi Sad, Trg Dositeja Obradovića 6, Novi Sad, Serbia, tel: ++381 21 485 2248, e – mail: borisbrkic93@uns.ac.rs

In this paper we study earthquake response of two adjacent structures with viscoelastic passive dampers and a friction damper, which is positioned between the structures in order to increase energy dissipation and to prevent pounding.

2. DESCRIPTION OF PROBLEM

We analyze dynamics of the system of two structures interconnected by the friction damper. Each of them consists of one rigid block representing the base, and another one which can slide without friction along the base, see Figure 1. The upper blocks are connected to the bases via viscoelastic rods, while they are connected by a friction damper to each other. During horizontal ground motion the bases move together with the ground. Upper blocks slide along the lower ones deforming the viscoelastic rods and dissipating the energy which is brought into the system during an earthquake. In some cases the friction damper is activated and energy also dissipates by dry friction, while upper blocks move relatively to each other.

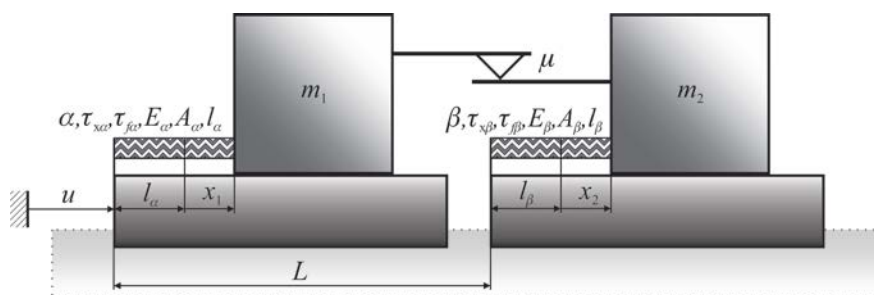


Figure 1. Mechanical system

At the beginning the system is at rest. At certain time instant the ground starts to move horizontally. Similar problem was treated in [10], where the simplified earthquake excitation was taken in the form of the product of a trigonometric and an exponential envelope function. In this paper we reexamine that problem describing horizontal ground motion by the Ricker's wavelet, which is frequently employed to model seismic data, see [11].

Masses of the upper blocks are denoted by m_1 and m_2 , while u stands for the movement of the bases. Relative movement of the upper blocks with respect to the lower ones is denoted by x_1 and x_2 , which at the same time represent elongations of the viscoelastic rods. Initial lengths of the rods, in undeformed state, are l_α and l_β . The gap between upper blocks is denoted by ξ , where $\xi=0$ indicates undesirable pounding. Forces in viscoelastic rods are presented by f_1 and f_2 , while n_1 and n_2 stand for the normal contact forces between upper and lower blocks, see a free body diagram in Figure 2. The friction force and the normal contact force within the friction damper are denoted by q and N . We assume uniaxial deformation of the viscoelastic rods and translatory motion of the upper blocks.

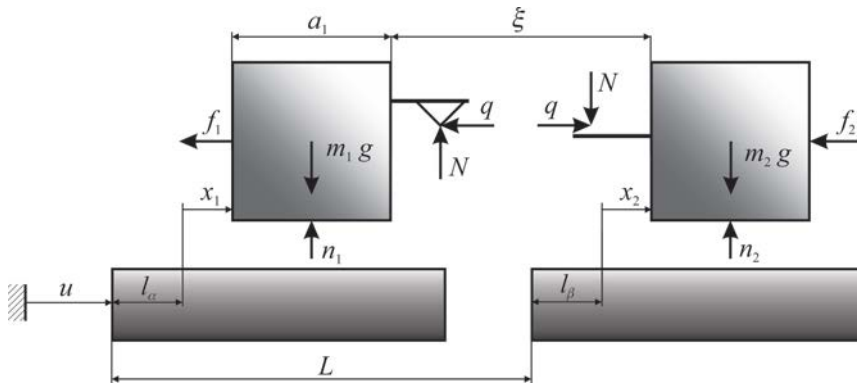


Figure 2. Free body diagram

Differential equations of motion and constitutive equations of the viscoelastic rods in the form of the fractional Zener model, read

$$m_1 (u^{(2)} + x_1^{(2)}) = -f_1 - q, \tag{1}$$

$$m_2 (u^{(2)} + x_2^{(2)}) = -f_2 + q, \tag{2}$$

$$f_1 + \tau_{f\alpha} f_1^{(\alpha)} = \frac{E_\alpha A_\alpha}{l_\alpha} (x_1 + \tau_{x\alpha} x_1^{(\alpha)}), \tag{3}$$

$$f_2 + \tau_{f\beta} f_2^{(\beta)} = \frac{E_\beta A_\beta}{l_\beta} (x_2 + \tau_{x\beta} x_2^{(\beta)}), \tag{4}$$

where $(*)^{(\gamma)} = d^\gamma(*)/dt^\gamma$, $A_\alpha, A_\beta, E_\alpha, E_\beta$ stand for cross-sectional areas and moduli of elasticity of viscoelastic rods. Viscoelastic model constants $\tau_{f\gamma}, \tau_{x\gamma}$ and E_α must satisfy inequalities $\tau_{x\gamma} > \tau_{f\gamma}, \tau_{f\gamma} > 0$, and $E_\gamma > 0$, according to the second law of thermodynamics, where $0 < \gamma < 1, \gamma \in \{\alpha, \beta\}$. Fractional derivatives of viscoelastic forces end elongations of the rods are taken in the Riemann-Liouville form, see [12].

The friction force q in the set-valued form reads

$$q \in \begin{cases} \mu N, & x_1^{(1)} - x_2^{(1)} > 0 \\ \mu N [-1, 1], & x_1^{(1)} - x_2^{(1)} = 0 \\ -\mu N, & x_1^{(1)} - x_2^{(1)} < 0, \end{cases} \tag{5}$$

where μ denotes the friction coefficient, see [13]. Earthquake excitation is modeled by the simplified model based on Ricker's wavelet, [11]

$$u(t) = u_0 \cdot \sum_{i=1}^l (2u_i - 1) e^{-u_i}, \quad u_i = \left[\frac{\pi (t - t_{si})}{t_{pi}} \right]^2, \quad (6)$$

where t_{pi} and t_{si} determine the shape of the wave function $u(t)$.

By solving the system of equations (1)-(6) using homogeneous initial conditions

$$x_1(0) = x_2(0) = x_1^{(1)}(0) = x_2^{(1)}(0) = f_1(0) = f_2(0) = 0, \quad (7)$$

the motion of the upper blocks can be obtained, together with the forces in viscoelastic rods and the friction force. The gap between the upper blocks $\xi = L + l_\beta + x_2 - l_\alpha - x_1 - a_1$ must be positive during the motion in order to avoid pounding.

Within the framework of the preparation for numerical integration of the posed system of equations, it is useful to describe the problem in dimensionless form. In order to do that, following nondimensional quantities are introduced, like in [14]

$$\bar{x}_i = \frac{x_i E_\alpha A_\alpha}{l_\alpha m_1 g}, \quad \bar{\xi} = \frac{\xi E_\alpha A_\alpha}{l_\alpha m_1 g}, \quad \bar{t} = t \sqrt{\frac{E_\alpha A_\alpha}{l_\alpha m_1}}, \quad \bar{f}_i = \frac{f_i}{m_1 g}, \quad \bar{q} = \frac{q}{m_1 g}, \quad \bar{\rho} = \frac{m_1}{m_2}, \quad (8)$$

$$\bar{\tau}_{f\alpha} = \tau_{f\alpha} \left(\frac{E_\alpha A_\alpha}{l_\alpha m_1} \right)^{\alpha/2}, \quad \bar{\tau}_{x\alpha} = \tau_{x\alpha} \left(\frac{E_\alpha A_\alpha}{l_\alpha m_1} \right)^{\alpha/2}, \quad \bar{\varepsilon} = \frac{A_\beta E_\beta}{A_\alpha E_\alpha}, \quad \bar{u} = \frac{u E_\alpha A_\alpha}{l_\alpha m_1 g}, \quad (i=1,2).$$

When the bar is omitted, the system of dimensionless equations, together with the initial conditions and restrictions, reads

$$\begin{aligned} x_1^{(2)} + u^{(2)} &= -f_1 - q, \\ x_2^{(2)} + u^{(2)} &= \rho(-f_2 + q), \\ f_1 + \tau_{f\alpha} f_1^{(\alpha)} &= x_1 + \tau_{x\alpha} x_1^{(\alpha)}, \\ f_2 + \tau_{f\beta} f_2^{(\beta)} &= \varepsilon(x_2 + \tau_{x\beta} x_2^{(\beta)}), \\ q &\in \begin{cases} \mu, & x_1^{(1)} - x_2^{(1)} > 0 \\ \mu[-1, 1], & x_1^{(1)} - x_2^{(1)} = 0 \\ -\mu, & x_1^{(1)} - x_2^{(1)} < 0, \end{cases} \quad (9) \\ x_1(0) = x_2(0) = x_1^{(1)}(0) = x_2^{(1)}(0) &= f_1(0) = f_2(0) = 0, \\ \tau_{f\gamma} > 0, \tau_{x\gamma} > \tau_{f\gamma}, 0 < \gamma < 1, \gamma &\in \{\alpha, \beta\}. \end{aligned}$$

The posed system contains second order differential equations and fractional differential equations, where the friction force is described by the non-smooth function.

3. NUMERICAL SOLUTION

Dealing with a non-smooth fractional order system is a complex task, see [15]. Due to non-smooth nature of the problem, there are three different motion phases, which are characterized by different sets of equations. Numerical treatment including a combinatorial analysis, as in [10], is used in order to find the solution of the posed problem, where the horizontal ground excitation is described by the Ricker's waves. Following sets of equations describe the system response during different motion phases. Time is discretized as $t_m = m\kappa$, ($m=0,1,2,\dots$) by introducing the time step κ . Numerical algorithm for calculation of forces in viscoelastic rods and relative coordinates of upper blocks during sliding phases reads

$$\begin{aligned}
 f_{1m} &= \frac{1}{1 + \tau_{f\alpha} h^{-\alpha}} \left\{ x_{1m} (1 + \tau_{x\alpha} h^{-\alpha}) + h^{-\alpha} \sum_{j=1}^m \left[\omega_j^\alpha (\tau_{x\alpha} x_{1m-j} - \tau_{f\alpha} f_{1m-j}) \right] \right\}, \\
 f_{2m} &= \frac{\varepsilon}{1 + \tau_{f\beta} h^{-\alpha}} \left\{ x_{2m} (1 + \tau_{x\beta} h^{-\beta}) + h^{-\beta} \sum_{j=1}^m \left[\omega_j^\beta \left(\tau_{x\beta} x_{2m-j} - \frac{\tau_{f\beta}}{\varepsilon} f_{2m-j} \right) \right] \right\}, \quad (10) \\
 x_{1m+1} &= 2x_{1m} - x_{1m-1} - h^2 (u_m^{(2)} + f_{1m} + q_m), \\
 x_{2m+1} &= 2x_{2m} - x_{2m-1} + h^2 \left[-u_m^{(2)} + \rho (-f_{2m} + q_m) \right], \quad (m > 0),
 \end{aligned}$$

where dimensionless friction force q_m has the value either μ or $-\mu$, according to (9)₅, while the Riemann-Liouville fractional derivative can be approximated by the Grünwald-Letnikov definition, see [10]. Coefficients ω_j^γ are calculated by

$$\omega_0^\gamma = 1, \quad \omega_j^\gamma = \left(1 - \frac{\gamma + 1}{j} \right) \omega_{j-1}^\gamma, \quad (j = 1, 2, 3, \dots), \quad (11)$$

and $u_m^{(2)} = u^{(2)}(m\kappa)$.

During the stick phase, relative positions of the upper blocks and the friction force are calculated by the following algorithm

$$\begin{aligned}
 x_{1m+1} &= 2x_{1m} - x_{1m-1} - h^2 \left[u_m^{(2)} + \frac{\rho}{\rho + 1} (f_{1m} + f_{2m}) \right], \\
 x_{2m+1} &= x_{1m+1} - c, \\
 q_m &= \frac{\rho f_{2m} - f_{1m}}{\rho + 1}, \quad (m > 0),
 \end{aligned} \quad (12)$$

where $x_{10} = x_{20} = f_{10} = f_{20} = x_{11} = x_{21} = 0$, according to the initial conditions (9)₆. During the stick phase, where $x_1^{(1)} - x_2^{(1)} = 0$, the value c is constant, i.e. $c = x_1 - x_2 = \text{const}$. Also, the friction force is calculated by (12)₃, unlike the sliding phases, where its has constant value μ or $-\mu$. Results of the numerical simulation are presented in the next section.

4. RESULTS AND DISCUSSION

Results of the simulation of motion are presented for the following values of ground motion parameters: $u_0=0.5$, $t_{p1}=1.25$, $t_{s1}=1.5$, $t_{p2}=1$, $t_{s2}=2$, $t_{p3}=2$, $t_{s3}=3$, $t_{p4}=3.5$, $t_{s4}=4$, $t_{p5}=3.8$, $t_{s5}=5$, parameters of the viscoelastic bodies: $\alpha=0.23$, $\tau_{\alpha}=1.183$, $\tau_{\beta}=0.004$, $\beta=0.53$, $\tau_{\gamma}=4$, $\tau_{\delta}=0.2$, friction coefficient $\mu=0.25$, $\varepsilon=2$, $\rho=1$, time step $\kappa=0.002$. Horizontal ground acceleration $u^{(2)}$ derived from (6) and for the chosen values of parameters is shown in Figure 3.

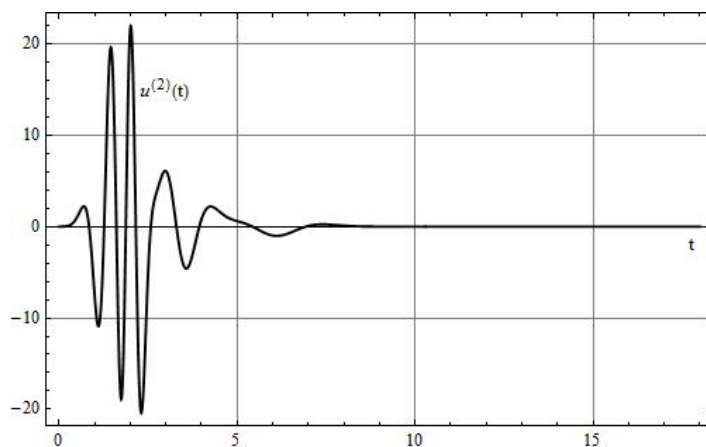


Figure 3. Horizontal ground excitation - Ricker's waves

Relative positions of upper blocks with respect to the base, $x_1(t)$ and $x_2(t)$, together with ground position $u(t)$, are presented in Figure 4, while relative velocities, $v_1(t)=x_1^{(1)}(t)$ and $v_2(t)=x_2^{(1)}(t)$ are given in Figure 5. The system starts its motion in the stick phase.

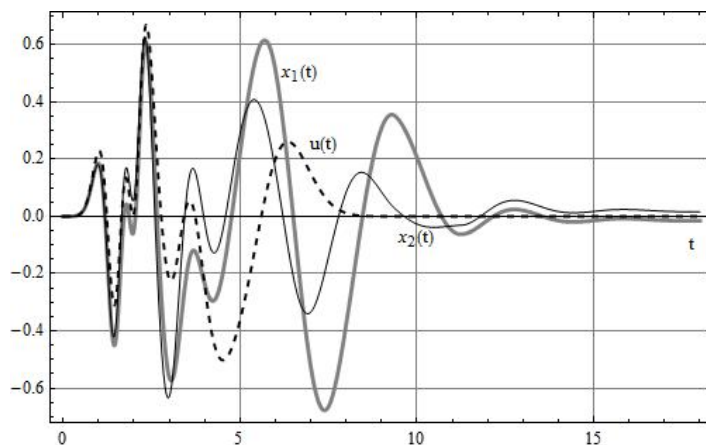


Figure 4. Relative positions $x_1(t)$, $x_2(t)$ and ground position $u(t)$

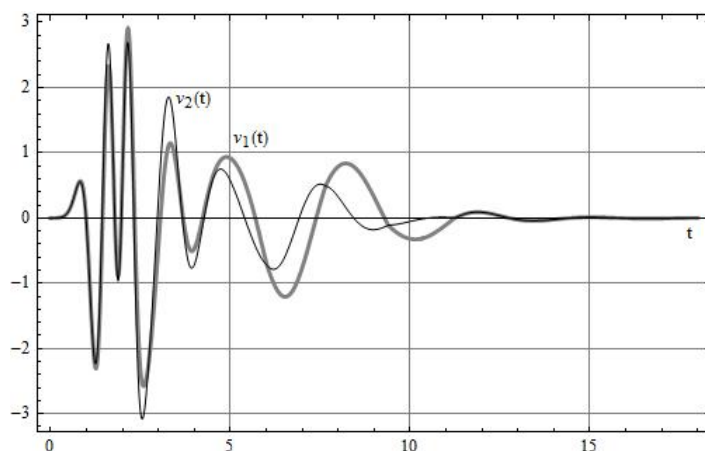


Figure 5. Relative velocities of upper blocks $v_1(t)$ and $v_2(t)$

Upper blocks move as one rigid body from the initial time instant until the friction force reaches its limiting value μ , when sliding occurs. The difference between relative velocities, $v_1(t) - v_2(t)$, and the friction force $q(t)$ are presented in Figure 6. Slip to the right and to the left alternates until approximately $t=11.2$ dimensionless units. The friction force jumps from one limiting value to another one when sliding changes direction. At about $t=11.2$ the stick phase occurs again. After that time instant the excitation is sufficiently small and the system remains in the stick phase. During that last phase the friction force is continuous function of time, and it is calculated by (12)₃.

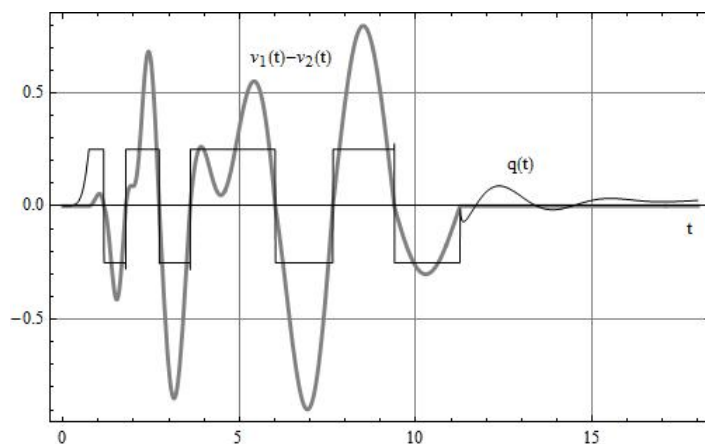


Figure 6. Relative velocity within friction element $v_1(t) - v_2(t)$ and friction force $q(t)$

Forces in viscoelastic rods, $f_1(t)$ and $f_2(t)$, are shown in Figure 7, while the gap $\xi(t)$ is presented in Figure 8. The gap $\xi(t)$ is positive all the time so pounding does not occur.

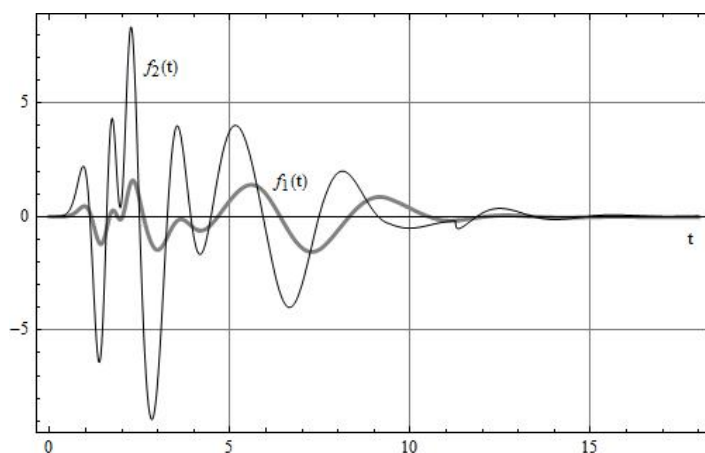


Figure 7. Forces in the viscoelastic dampers $f_1(t)$ and $f_2(t)$

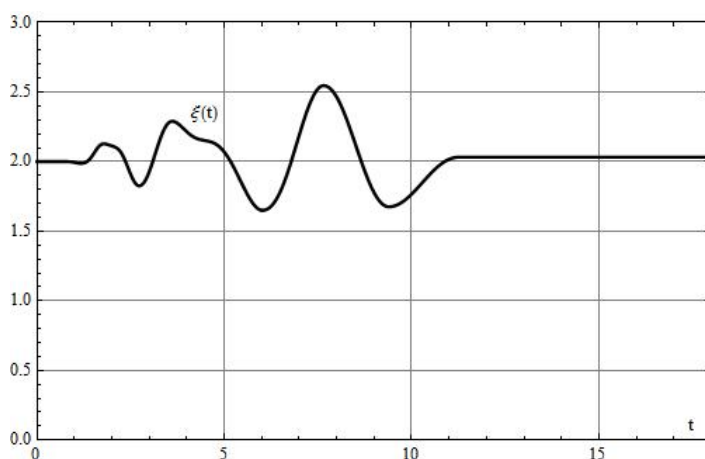


Figure 8. Distance between upper blocks $\xi(t)$ during motion

5. CONCLUDING REMARKS

Dynamics response of adjacent structures to a simplified horizontal seismic excitation in the form of Ricker's waves is considered, Figure 1. The non-smooth mechanical system is described by the set of the second order differential equations and fractional order differential equations in dimensionless form, together with the initial conditions and restrictions to the model parameters, see (9). In order to obtain the solution, numerical algorithm is formed (10)-(12), taking into account combinatorial analysis due to phase changes, see [10]. Results are presented for chosen values of system parameters, Figures 4-8, for which pounding does not take place. Instead of the simplified ground excitation

described by (6), it would be interesting to analyze the response of the system to real earthquake excitations.

Acknowledgements

Funding for this work was partially provided by the Faculty of Technical Sciences of the University of Novi Sad, Project No2018-054.

REFERENCES

- [1] Kasai, K.: Building pounding damage during the 1989 Loma Prieta earthquake. *Engineering Structures*, **1997.**, vol. 19, № 3, p.p. 195-207.
- [2] Dobre, D., Dragomir, C.S., Georgescu, E.S. : Pounding effects during an earthquake, with and without consideration of soil-structure interaction. *Second European Conference on Earthquake Engineering and Seismology*, Istanbul, Turkey, **2014**.
- [3] Sotysk, B., Jankowski, R.: Building damage due to structural pounding during earthquakes. *Journal of Physics: Conference Series* 628, 012040, Auckland, New Zealand, **2015**.
- [4] Crozet, V., Politopoulos, I., Yang, M., Martinez, J-M., Erlicher, S.: Influential structural parameters of pounding between buildings during earthquakes. *Procedia Engineering*, **2017.**, vol. 199, p.p. 1092–1097.
- [5] Elwardany, H., Seleemah, A., Jankowski, R.: Seismic pounding behavior of multi-story buildings in series considering the effect of infill panels. *Engineering Structures*, **2017**, vol. 144, p.p. 139–150.
- [6] Soltysik, B., Falborski, T., Jankowski, R.: Preventing of earthquake-induced pounding between steel structures by using polymer elements – experimental study. *Procedia Engineering*, **2017**, vol. 199, p.p. 278–283.
- [7] Dimitrakopoulos, E. G., Makris, N., Kappos, A. J.: Dimensional analysis of the earthquake-induced pounding between adjacent structures. *Earthquake Engineering and Structural Dynamics*, **2009**, vol. 38, № 7, p.p. 867-886.
- [8] Mate, N.U., Bakre, S.V., Jaiswal, O.R.: Comparative study of impact simulation models for linear elastic structures in seismic pounding. *Proceedings of the Fifteenth World Conference on Earthquake Engineering*, Lisbon, Portugal, **2012**.
- [9] Qichao, X., Jingcai, Zh., Jian, H., Chunwei, Zh., Guangping, Z.: Seismic control performance for pounding tuned mass damper based on viscoelastic pounding force analytical method. *Journal of Sound and Vibration*, **2017.**, vol. 411, p.p. 362–377.
- [10] Zigic, M., Grahovac, N.: Earthquake response of adjacent structures with viscoelastic and friction dampers. *Theoretical and Applied Mechanics*, **2015.**, vol. 42, № 4, p.p. 277-289.
- [11] Ricker, N.H.: Transient waves in visco-elastic media. Elsevier, Amsterdam, **1977**.
- [12] Samko S.G., Kilbas A.A., Marichev O.I.: *Fractional integrals and derivatives*, Gordon and Breach Sci. Publishers, Yverdon, **1993**.
- [13] Glocker Ch. : *Set-valued force laws*, Springer, Berlin, **2001**.

- [14] Zigic M.: *Seismic response of a column like structure with both fractional and dry friction type of dissipation* (in Serbian). Ph.D. thesis, Faculty of Technical Sciences, Novi Sad, Serbia, **2012**.
- [15] Grahovac N., Zigic M., Spasic D.: On Impact Scripts with Both Fractional and Dry Friction Type of Dissipation, *Int. J. Bifurcation Chaos Appl. Sci. Eng.*, **2012.**, vol. 22, № 4., Paper № 1250076 (10 pages).

ДИНАМИКА СУСЕДНИХ КОНСТРУКЦИЈА ТОКОМ ХОРИЗОНТАЛНОГ КРЕТАЊА ТЛА

Резиме: У овом раду проучене су две конструкције које су међусобно повезане фрикционим елементом. Обе конструкције састоје се од два блока и вискоеластичног пригушивача, који је моделиран фракционим Зенеровим моделом. Сила трења унутар фрикционог елемента описана је вишевердносим Кулоновим законом силе трења. Хоризонтално кретање тла узрокује кретање обе конструкције што може довести до њиховог судара са разарајућим ефектом. Енергија доведена у систем који се састоји од две конструкције повезане фрикционим пригушивачем, расипа се радом сила у вискоеластичним штаповима и радом силе трења. Хоризонтално кретање подлоге моделирано је поједностављеним моделом земљотреса који укључује Рикерове сеизмичке таласе.

Кључне речи: суседне конструкције, земљотрес, суво трење, висоеластичност